

On a new type of divergence for spiky Wilson loops and related entanglement entropies

Harald Dorn ¹

*Institut für Physik und IRIS Adlershof, Humboldt-Universität zu Berlin,
Zum Großen Windkanal 6, D-12489 Berlin, Germany*

Abstract

We study the divergences of Wilson loops for a contour with a cusp of zero opening angle, combined with a nonzero discontinuity of its curvature. The analysis is performed in lowest order, both for weak and strong coupling. Such a spike contributes a leading divergent term proportional to the inverse of the square root of the cutoff times the jump of the curvature. As nextleading term appears a logarithmic one in the supersymmetric case, but it is absent in QCD. The strong coupling result, obtained from minimal surfaces in AdS via holography, can be used also for applications to entanglement entropy in (2+1)-dimensional CFT's.

¹dorn@physik.hu-berlin.de

1 Introduction

Wilson loops for smooth contours in non-supersymmetric gauge theories, besides a linear divergence proportional to the length, do not require any further renormalisation beyond that of the coupling constant [1, 2]. For the local supersymmetric generalisation in $\mathcal{N} = 4$ super Yang-Mills [3, 4] the situation is even more comfortable: the coupling is not renormalised, and the linear divergence cancels between the gauge boson and scalar contribution [5].

For contours with cusps or self-intersections each of these singular points generates renormalisation Z-factors [1, 6]. The corresponding cusp anomalous dimension depends on the cusp angle ² ϑ and the coupling constant and has been calculated in the 80-ies up to perturbative two loop level [1, 7, 8]. Later on it turned out to be related to various other physical situations, and with the advent of AdS-CFT holography it became one of the most studied quantities from both the weak as well as the strong coupling side. It is now available up to three loops both for $\mathcal{N} = 4$ SYM and QCD [9, 10]. For strong coupling one has the leading and next leading contribution [5, 11]. Of special interest is also the limit of large imaginary angle [8]. It plays a crucial role for scattering amplitudes and the dimensions of large spin operators, and using techniques of integrability even an interpolation between weak and strong coupling has been found [12, 13].

The minimal string surfaces, one has to consider for the strong coupling evaluation, play still another prominent role. They carry all the information needed for the strong coupling evaluation of entanglement entropies via holography in (2+1)-dimensional conformal field theories [14, 15]. The cusp anomalous dimension appears then as the coefficient of the logarithmic divergence due to a cusp in the boundary of a subregion in 2-dimensional static space. In the following we mainly use the Wilson loop language, translations into the context of entanglement entropy should be straightforward.

Besides the already mentioned limit for infinite imaginary angle, the limits $\vartheta \rightarrow 0$ and $\vartheta \rightarrow \pi$ have been studied in detail. The first limit corresponds to the approach to a smooth contour, and therefore the cusp anomalous dimension vanishes. Its approach to zero is of quadratic order in ϑ , with a coefficient related to the Bremsstrahlung of a heavy charge [16]. In the other limit the cusp anomalous dimension diverges proportional to $1/(\pi - \vartheta)$ with a coefficient, which can be identified with the static quark-antiquark potential on the sphere [9], for a related statement see also [17].

If one looks at the lowest order Feynman diagrams responsible for the cusp logarithmic divergence, one realises that this divergence is absent if one puts $\vartheta = \pi$ before the removal of the regularisation, i.e. the limit $\vartheta \rightarrow \pi$ does not commute with renormalisation [18].

$\vartheta = \pi$ corresponds to a jump of the tangent vector of the contour to its additive inverse. One situation, where this is relevant, appears for a contour which runs on a piece forward and backward and is connected to the issue of zigzag symmetry [5, 19].

Our main interest in this paper concerns the case, for which one has $\vartheta = \pi$ and a finite nonzero jump in the curvature of the contour, i.e. a case where the cusp

²With the convention: opening angle is $\pi - \vartheta$.

degenerates to a spike.³ ⁴ We will find a new type of divergence which depends on the jump in curvature. In this respect the $\vartheta = \pi$ case is very special, because for $0 \leq \vartheta < \pi$ any dependence of the divergence on other local quantities beyond ϑ has been excluded, both in small coupling perturbation theory [18] as well as in the holographic treatment for strong coupling [21].

In the following section 2 we consider the lowest order for weak coupling, both for QCD and $\mathcal{N} = 4$ SYM. Section 3 is devoted to a study of minimal surfaces in AdS, relevant for the strong coupling behaviour in $\mathcal{N} = 4$ SYM. After the concluding section 4 the paper is completed by some technical appendices.

2 Lowest order perturbation theory

The Euclidean local supersymmetric Wilson loop for a closed contour parameterised by $x^\mu(\sigma)$ is given by [3–5]

$$W = \frac{1}{N} \langle \text{tr } P \exp \int (iA_\mu \dot{x}^\mu + |\dot{x}| \phi_I \theta^I) d\sigma \rangle . \quad (1)$$

The coupling to the scalars ϕ_I is controlled by a contour $\theta^I(\sigma)$ on S^5 . Here we restrict ourselves to constant θ^I . The extension to nontrivial contours and cusps or spikes on S^5 would be straightforward. In the non-supersymmetric case the scalars are absent. The divergence of interest for QCD is given by the two diagrams in figure 1. In the supersymmetric case the analog diagrams with scalar propagator have to be added.

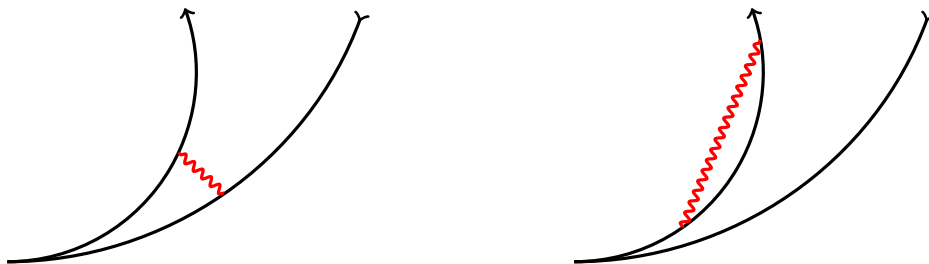


Figure 1: *The lowest order gluon diagrams contributing to the spike divergence. The contour near the spike is shown in black with arrows pointing to increasing contour parameter. Red wavy lines are gluon propagators.*

At this point a comment is in order, explaining why the right diagram is included and why in contrast the analogue for the other leg of the spike is not included. The

³Our interest in this situation has been triggered by a recent paper which studies a different type of spikes, those built by spirals [20].

⁴To fix nomenclature, following parts of the physical literature, we use the word cusp for a corner with nonzero opening angle $(\pi - \vartheta)$ and spike for a cusp with zero opening angle.

diagrams with both ends of the propagator on one and the same smooth piece of the contour generate a logarithmic end point contribution. It has to be attributed to the endpoint belonging to the smaller value of the contour parameter σ .⁵ For the right diagram in figure 1 this point is the tip of our spike under consideration, for the analogue on the other leg it would be the foregoing cusp or spike.

A convenient setting for discussing all the renormalisation issues of the non-local Wilson operators in the language of local objects is provided by the use of an one dimensional auxiliary field living on the contour, for a review see [18] and references therein.

The starting point for the analysis of the contribution of the spike to the divergences is then (g coupling, C_F quadratic Casimir for the fundamental representation of $SU(N)$ and $+\dots$ for order g^2 contributions from outside a vicinity of the spike)

$$\log W = \frac{g^2 C_F}{4\pi^2} \left(I_{\text{sc}}^{\text{sp}} + I_{\text{sc}}^{\text{end}} - I_{\text{gl}}^{\text{sp}} - I_{\text{gl}}^{\text{end}} + \dots \right) + \mathcal{O}(g^4), \quad (2)$$

with

$$I_{\text{sc}}^{\text{sp}} = \int^{\sigma_s} d\sigma_1 \int_{\sigma_s} d\sigma_2 \frac{1}{D_{1,2}}, \quad I_{\text{sc}}^{\text{end}} = \int_{\sigma_s} d\sigma_2 \int_{\sigma_s}^{\sigma_2} d\sigma_1 \frac{1}{D_{1,2}}, \quad (3)$$

$$I_{\text{gl}}^{\text{sp}} = \int^{\sigma_s} d\sigma_1 \int_{\sigma_s} d\sigma_2 \frac{\dot{\vec{x}}_1 \dot{\vec{x}}_2}{D_{1,2}}, \quad I_{\text{gl}}^{\text{end}} = \int_{\sigma_s} d\sigma_2 \int_{\sigma_s}^{\sigma_2} d\sigma_1 \frac{\dot{\vec{x}}_1 \dot{\vec{x}}_2}{D_{1,2}}, \quad (4)$$

$$D_{1,2} = (\vec{x}(\sigma_1) - \vec{x}(\sigma_2))^2 + a^2. \quad (5)$$

For UV regularisation we have introduced the parameter a . As contour parameter has been chosen the geometrical length, i.e. $|\dot{x}| = 1$, σ_s is its value at the tip of the spike.

The expansion of $\vec{x}(\sigma_1)$ and $\vec{x}(\sigma_2)$ near the tip of the spike for the left diagram in fig.1 is

$$\begin{aligned} \vec{x}(\sigma_1) &= \vec{x}(\sigma_s) + \vec{t}(\sigma_1 - \sigma_s) + \vec{k}_1 \frac{(\sigma_1 - \sigma_s)^2}{2} + \dots, \quad \sigma_1 \leq \sigma_s, \\ \vec{x}(\sigma_2) &= \vec{x}(\sigma_s) - \vec{t}(\sigma_2 - \sigma_s) + \vec{k}_2 \frac{(\sigma_2 - \sigma_s)^2}{2} + \dots, \quad \sigma_2 \geq \sigma_s. \end{aligned} \quad (6)$$

The appearance of \vec{t} and $-\vec{t}$ in the first and second line is due to our choice $\vartheta = \pi$ for the cusp angle. For the right diagram the expansion looks similar, but instead of $-\vec{t}$ in the second line one has $+\vec{t}$ and both σ_1 and σ_2 are larger then σ_s .

This implies for the nominators in (4): $\mp 1 + \mathcal{O}(\sigma_1 - \sigma_2)$ for the first and second integral, respectively. The order $\mathcal{O}(\sigma_1 - \sigma_2)$ does not contribute to divergences for $a \rightarrow 0$, hence

$$I_{\text{gl}}^{\text{sp}} = -I_{\text{sc}}^{\text{sp}} + \mathcal{O}(a^0), \quad I_{\text{gl}}^{\text{end}} = I_{\text{sc}}^{\text{end}} + \mathcal{O}(a^0). \quad (7)$$

⁵In QCD these end point contributions are responsible for an anomalous dimension of Wilson operators for *open* contours [22–25].

We now discuss the calculation of the divergent part of $I_{\text{sc}}^{\text{sp}}$, the end point integral can be taken from the literature. After changing variables $\sigma_1 - \sigma_s = -\tau_1$, $\sigma_2 - \sigma_s = \tau_2$ and introducing polar coordinates in the (τ_1, τ_2) -plane we get

$$I_{\text{sc}}^{\text{sp}} = \int_0^l \frac{dr}{r} \int_0^{\pi/2} d\varphi \frac{1}{1 - \sin 2\varphi + \frac{r^2}{4} (\vec{k}_1 \cos^2 \varphi - \vec{k}_2 \sin^2 \varphi)^2 + a^2/r^2} + \mathcal{O}(a^0). \quad (8)$$

Here use has been made of $\vec{t} \cdot \vec{k}_j = 0$ for $j = 1, 2$. The $\mathcal{O}(a^0)$ takes notice of finite terms arising from higher terms in the expansion of $\vec{x}(\sigma)$. l is an auxiliary parameter defining a certain vicinity of the spike, it has no effect on the divergent terms.

The further evaluation of this integral is performed in appendix A, and from there we get

$$I_{\text{sc}}^{\text{sp}} = \frac{\sqrt{\pi} (\Gamma(1/4))^2}{2 \sqrt{2a} |\vec{k}_1 - \vec{k}_2|} + \log a + \mathcal{O}(a^0). \quad (9)$$

For the total spiky contribution to the divergence, we have to combine this with the known

$$I_{\text{sc}}^{\text{end}} = \frac{\pi l}{2a} + \log a + \mathcal{O}(a^0). \quad (10)$$

The $1/a$ -term is the contribution to the well-known overall linear divergence proportional to the length of the contour. It has nothing to do with the effect of the spike. Then, putting together (2),(7),(9),(10), we get for the contribution of the spike to the Wilson loop in QCD

$$\log W_{\text{QCD}} \Big|_{\text{spiky}} = \frac{g^2 C_F}{4\pi^2} \left(\frac{\sqrt{\pi} (\Gamma(1/4))^2}{2 \sqrt{2a} |\vec{k}_1 - \vec{k}_2|} + \mathcal{O}(a^0) \right) + \mathcal{O}(g^4). \quad (11)$$

For the supersymmetric case and smooth path on S^5 one finds instead

$$\log W_{\text{SYM}} \Big|_{\text{spiky}} = \frac{g^2 C_F}{4\pi^2} \left(\frac{\sqrt{\pi} (\Gamma(1/4))^2}{\sqrt{2a} |\vec{k}_1 - \vec{k}_2|} + 2 \log a + \mathcal{O}(a^0) \right) + \mathcal{O}(g^4). \quad (12)$$

The absence of a logarithmic term in QCD and its presence in SYM we interpret as somehow related to the presence or absence of zig-zag symmetry.

In dimensional regularisation the logarithmic term corresponds as usual to a pole at dimension 4. The $1/\sqrt{a}$ term corresponds to a pole at dimension 3.5.

3 Holographic evaluation for strong coupling

For large N and strong 't Hooft coupling $\lambda = g^2 N$ in $\mathcal{N} = 4$ SYM one has the holographic formula [4]

$$\log W = - \frac{\sqrt{\lambda}}{2\pi} A, \quad (13)$$

with A denoting the area of the minimal surface in AdS approaching the Wilson loop contour on the boundary.

For the application to entropies in $(2+1)$ -dimensional CFT's this area gives at strong coupling up to a factor the entanglement of the two-dimensional region enclosed by the contour [14, 15].

We do not attempt to solve the difficult task of finding the minimal surface for the generic spike situation, discussed in the previous section. Instead we generate a special spiky situation by conformal transformation of a well-known explicit solution, that for the case of two parallel straight lines [4].⁶ Putting these two lines away from the origin of our coordinates, after inversion on the origin we get two circles of different radius, touching each other at one point. This procedure yields a contour with two spikes with common tips. The small subtleties for the comparison with the results in section 2, due to this touching of the two tips, will be discussed in appendix C. The situation is illustrated in Figure 2.

Let us now consider the two parallel straight lines of distance L , located parallel to the x_1 axis and crossing the x_2 axis at $x_2 = M \pm L/2$, ($M - L/2 > 0$). In Poincaré coordinates (x_1, x_2, z) , with $z = 0$ as boundary, $ds^2 = (dz^2 + dx_1^2 + dx_2^2)/z^2$ the related minimal surface is given by [4]

$$\begin{aligned} z(\sigma, \tau) &= r(\sigma) , & \sigma &\in (-L/2, L/2) , \quad \tau \in (-\infty, \infty) , \\ x_1(\sigma, \tau) &= \tau , & x_2(\sigma, \tau) &= M + \sigma . \end{aligned} \quad (14)$$

The function $r(\sigma)$ is defined via

$$r(-\sigma) = r(\sigma) \quad \text{and} \quad \sigma = r_0 \int_{\frac{r(\sigma)}{r_0}}^1 \frac{y^2 dy}{\sqrt{1-y^4}} \quad \text{for } 0 < \sigma < \frac{L}{2} , \quad (15)$$

with

$$L = 2r_0 \int_0^1 \frac{y^2 dy}{\sqrt{1-y^4}} = \frac{(2\pi)^{3/2} r_0}{(\Gamma(\frac{1}{4}))^2} . \quad (16)$$

Now we apply the AdS isometry

$$x_\mu \mapsto \frac{x_\mu}{x^2 + z^2} , \quad z \mapsto \frac{z}{x^2 + z^2} , \quad (17)$$

which on the boundary just yields the conformal inversion on the origin. Then the image of (14) under (17) is

$$\begin{aligned} x_1 &= \frac{\tau}{\tau^2 + (M + \sigma)^2 + r^2(\sigma)} , \\ x_2 &= \frac{M + \sigma}{\tau^2 + (M + \sigma)^2 + r^2(\sigma)} , \\ z &= \frac{r(\sigma)}{\tau^2 + (M + \sigma)^2 + r^2(\sigma)} . \end{aligned} \quad (18)$$

⁶Conformal transformations of this case, combined with T-dualities have been studied recently in [26].

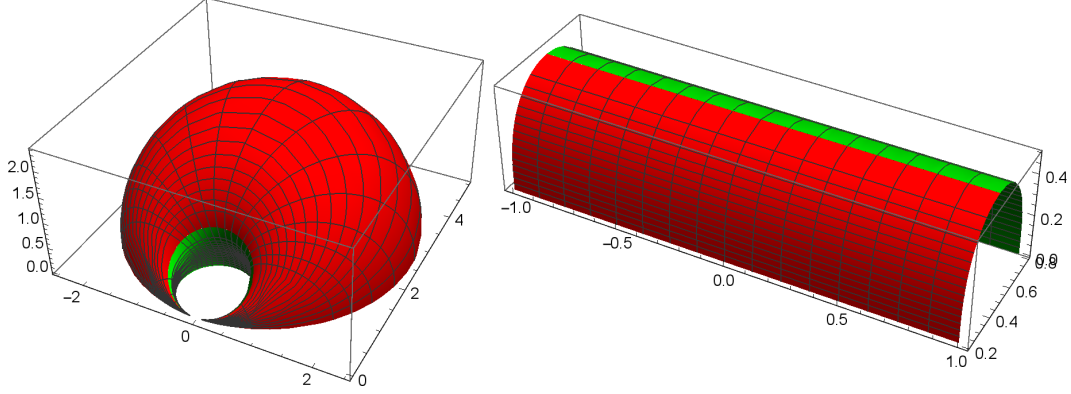


Figure 2: $r_0 = 0.5$, $M = 0.5$, note the different scales. The green and red pieces correspond to positive and negative values of σ , respectively.

Figure 2 shows both the original (right) and the image (left) for a special choice of M and r_0 .

The wanted regularised area A_ϵ is then given by cutting the surface (18) at $z = \epsilon$ and taking into account only the piece $z > \epsilon$. Since (17) inside AdS is an isometry, we can calculate this area also on the original surface (14) whose induced metric is simpler.

The boundary of the region on (14), which has to be taken into account, is then given by

$$\epsilon = \frac{r(\sigma)}{\tau^2 + (M + \sigma)^2 + r^2(\sigma)} . \quad (19)$$

Examples of the corresponding curves on (14) are shown in figure 3 for three different values of ϵ . The integration for A_ϵ is performed over all σ , τ for which the r.h.s.

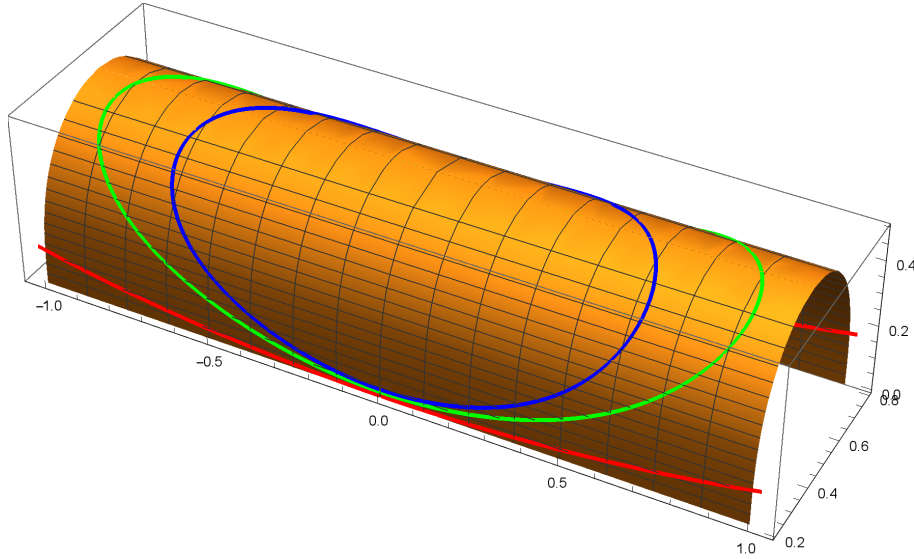


Figure 3: $r_0 = 0.5$, $M = 0.5$, red, green, blue: $\epsilon = 0.1, 0.4, 0.6$

of (19) is larger than ϵ . There is a maximum τ_ϵ^2 for allowed values of τ^2 . For

each given $\tau \in (-\tau_\epsilon, \tau_\epsilon)$ the boundaries for the σ -integration are denoted by $\sigma_\epsilon^\pm(\tau)$. The integrand, due to the induced metric on (14), is given by $\sqrt{1 + r'^2}/r^2$. This is independent of τ , and the corresponding conservation law allows to simplify to r_0^2/r^4 . Together this gives

$$A_\epsilon = A_\epsilon^+ + A_\epsilon^- , \quad (20)$$

$$\begin{aligned} A_\epsilon^+ &= r_0^2 \int_{-\tau_\epsilon}^{\tau_\epsilon} d\tau \int_0^{\sigma_\epsilon^+(\tau)} \frac{d\sigma}{r^4(\sigma)} , \\ A_\epsilon^- &= r_0^2 \int_{-\tau_\epsilon}^{\tau_\epsilon} d\tau \int_{\sigma_\epsilon^-(\tau)}^0 \frac{d\sigma}{r^4(\sigma)} . \end{aligned} \quad (21)$$

The separation into the contributions from positive and negative σ has been made because in the next step we want to change the integration variable from σ to r . Only for each piece separately the relation between σ and r is one to one.

With $\sigma(r) \geq 0$ defined in (15) we get

$$\frac{d\sigma}{dr} = - \frac{r^2}{r_0^2} \frac{1}{\sqrt{1 - (r/r_0)^4}} , \quad (22)$$

and with $r_\epsilon^\pm(\tau)$ defined by

$$\epsilon \tau^2 = r_\epsilon^\pm(\tau) - \epsilon \left((M \pm \sigma(r_\epsilon^\pm(\tau)))^2 + (r_\epsilon^\pm(\tau))^2 \right) \quad (23)$$

arrive at

$$A_\epsilon^\pm = \int_{-\tau_\epsilon}^{\tau_\epsilon} d\tau \int_{r_\epsilon^\pm(\tau)}^{r_0} \frac{dr}{r^2 \sqrt{1 - (r/r_0)^4}} . \quad (24)$$

These integrals and their behaviour for $\epsilon \rightarrow 0$ are discussed in some detail in appendix B. It results in (57), i.e.

$$A_\epsilon^\pm = \frac{\pi}{\epsilon(M \pm L/2)} - \frac{2(2\pi)^{3/4}}{\Gamma(\frac{1}{4})} \left(1 + \frac{\pi\sqrt{2\pi}}{(\Gamma(\frac{1}{4}))^2} \right) \frac{1}{\sqrt{\epsilon L}} + \mathcal{O}(\epsilon^0) . \quad (25)$$

To compare with the results in section 2, we have to relate L and M to the length of our contour and to the jump of the curvature at the spikes. The radii of the two circles are

$$R_{1|2} = \frac{1}{2(M \pm \frac{L}{2})} . \quad (26)$$

This implies for the circumferences l_1, l_2 and the jump in curvature

$$l_{1|2} = \frac{\pi}{M \pm \frac{L}{2}} , \quad |\vec{k}_1 - \vec{k}_2| = 2L . \quad (27)$$

Then with (25), (20) we get

$$A_\epsilon = \frac{l_1 + l_2}{\epsilon} - \frac{4\sqrt{2}(2\pi)^{3/4}}{\Gamma(\frac{1}{4})} \left(1 + \frac{\pi\sqrt{2\pi}}{(\Gamma(\frac{1}{4}))^2} \right) \frac{1}{\sqrt{\epsilon |\vec{k}_1 - \vec{k}_2|}} + \mathcal{O}(\epsilon^0) . \quad (28)$$

The usual $1/\epsilon$ divergence proportional to the length of the contour is not influenced by the presence of the spikes. Since we have two spikes, the $1/\sqrt{\epsilon}$ divergence to be attributed to *one* spike is half of the corresponding term in (28).

The holographic calculation is relevant for the supersymmetric case. Therefore, it is at first sight amazing that the divergence has no logarithmic piece, while for weak coupling there is one (12) (but not for QCD (11)).

In appendix C we show, that the weak coupling calculation for the contour of this section, with its two touching spikes, yields both for QCD and SYM no logarithmic term.

What concerns the divergence related a single spike it remains open, whether a logarithmic term present at weak coupling survives at strong coupling or has a coefficient approaching zero.

4 Conclusions

We have analysed the divergent contribution to Wilson loops (entanglement entropies) due to a class of spikes of the contour, those with cusp angle equal to π and with a nonzero jump of the curvature. For weak coupling the analysis has been done both for QCD and SYM. At strong coupling for $\mathcal{N} = 4$ SYM. Both for weak and strong coupling we found in lowest order a divergence proportional to the inverse square root of the product of the dimensionful short distance cutoff and the discontinuity of the curvature.

Let us identify the cutoffs for the weak and strong coupling case, i.e. $a = \epsilon$ and assume that also higher order corrections to the leading divergence are all $\propto 1/\sqrt{ak_{12}}$. Then we get

$$\log W_{\text{SYM}} \Big|_{\text{spiky}} = \frac{\Omega(\lambda)}{\sqrt{a} |\vec{k}_1 - \vec{k}_2|} + \Gamma_{\text{spike}}(\lambda) \log a + \mathcal{O}(a^0) . \quad (29)$$

The function $\Omega(\lambda)$ would be

$$\Omega(\lambda) = \lambda \frac{(\Gamma(1/4))^2}{2(2\pi)^{3/2}} + \mathcal{O}(\lambda^2) \quad (30)$$

and

$$\Omega(\lambda) = \sqrt{\lambda} \frac{2\sqrt{2}}{(2\pi)^{1/4}\Gamma(\frac{1}{4})} \left(1 + \frac{\pi\sqrt{2\pi}}{(\Gamma(\frac{1}{4}))^2}\right) + \dots \quad (31)$$

for small and large 't Hooft coupling, respectively. Use has been made of (12), (13) and one half of (28).

So far for $\Gamma_{\text{spike}}(\lambda)$ we have only the weak coupling behavior (12)

$$\Gamma_{\text{spike}}(\lambda) = \frac{\lambda}{2\pi^2} + \mathcal{O}(\lambda^2) . \quad (32)$$

Further study should confirm this picture by an analysis of next leading corrections. Then the most interesting question is, whether $\Omega(\lambda)$ and $\Gamma_{\text{spike}}(\lambda)$ are new

independent functions of the coupling or whether they are somehow related to known ones.⁷

For QCD we have for both functions the weak coupling results. $\Omega(\lambda)$ is then half of its partner for SYM and $\Gamma_{\text{spike}}(\lambda)$ is zero.

It would be interesting to study also cases with cusp angle $\vartheta = \pi$, $\vec{k}_1 = \vec{k}_2$ but a discontinuity in the third or higher derivative. Another straightforward generalisation concerns contours with additional discontinuities in the coupling to scalars on S^5 .

Ignoring all divergences other than logarithmic ones, or equivalently using dimensional regularisation, the function $\Omega(\lambda)$ plays no role in the definition of the renormalised Wilson loop and the analysis of its scaling behaviour via the renormalisation group. Then only $\Gamma_{\text{spike}}(\lambda)$ is of immediate interest. But in any case, for the application to entanglement entropy both functions $\Omega(\lambda)$ and $\Gamma_{\text{spike}}(\lambda)$ are of physical interest.

A last comment concerns a comparison with another case, in which the coefficient in front of a logarithmic divergence becomes singular. The holographic entanglement entropy for static regions in $(3+1)$ -dimensional CFT's has a logarithmic divergence. Its coefficient [27, 28] becomes singular, if the boundary of the spatial region develops conical singularities. The direct calculation for such singular boundaries yields a $\log^2 \epsilon$ divergences [29, 30]. This has to be contrasted with our case, where the transition to a stronger divergence yields $1/\sqrt{\epsilon}$.

Acknowledgement:

I would like to thank Nadav Drukker for a helpful discussion and Florian Loebbert for a hint concerning the figures.

⁷The lowest order of $\Gamma_{\text{spike}}(\lambda)$ exhibits an intriguing coincidence with that of the cusp anomalous dimension, defined in the context of large imaginary angle. But this can be an accident due to the simple arithmetic at this order.

Appendix A

Here we discuss the divergences for $a \rightarrow 0$ of the integral in (8), denoting it in this appendix by I

$$I(a, l, \vec{k}_1, \vec{k}_2) = \int_0^l \frac{dr}{r} \int_0^{\pi/2} d\varphi \frac{1}{1 - \sin 2\varphi + \frac{r^2}{4}(\vec{k}_1 \cos^2 \varphi - \vec{k}_2 \sin^2 \varphi)^2 + a^2/r^2} .$$

If $a \rightarrow 0$, $r \rightarrow 0$, the φ -integration becomes divergent at $\varphi = \pi/4$. Therefore, we put $\varphi = \pi/4 + \psi$ and can write I as

$$I(a, l, \vec{k}_1, \vec{k}_2) = \int_0^l \frac{dr}{r} \int_{-\pi/4}^{\pi/4} d\psi \frac{1}{\psi^2 g_0(\psi) + r^2 g_2(\psi) + a^2/r^2} , \quad (33)$$

with

$$g_0(\psi) = \frac{1 - \cos 2\psi}{\psi^2} = 2 + \mathcal{O}(\psi^2) , \quad (34)$$

$$\begin{aligned} g_2(\psi) &= \frac{1}{16} ((1 - \sin 2\psi)^2 \vec{k}_1^2 + (1 + \sin 2\psi)^2 \vec{k}_2^2 - 2 (\cos 2\psi)^2 \vec{k}_1 \vec{k}_2) \\ &= \frac{1}{16} (\vec{k}_1 - \vec{k}_2)^2 + \mathcal{O}(\psi) . \end{aligned} \quad (35)$$

To get the leading divergence one can replace $g_0(\psi)$ and $g_2(\psi)$ by their values at $\psi = 0$. But more care is necessary for the next-leading term, hence we continue with

$$I = I_1 + I_2 , \quad (36)$$

$$I_1 = \int_0^l \frac{dr}{r} \int_{-\pi/4}^{\pi/4} d\psi \frac{1}{\psi^2 g_0(0) + r^2 g_2(0) + a^2/r^2} , \quad (37)$$

$$I_2 = \int_0^l \frac{dr}{r} \int_{-\pi/4}^{\pi/4} d\psi \left(\frac{1}{\psi^2 g_0(\psi) + r^2 g_2(\psi) + a^2/r^2} - \frac{1}{\psi^2 g_0(0) + r^2 g_2(0) + a^2/r^2} \right) .$$

Let us start with I_2 . After $a/r = y$ we get

$$I_2 = \int_{a/l}^\infty \frac{dy}{y} \int_{-\pi/4}^{\pi/4} d\psi \frac{\psi^2(g_0(0) - g_0(\psi)) + \frac{a^2}{y^2}(g_2(0) - g_2(\psi))}{(\psi^2 g_0(\psi) + \frac{a^2}{y^2} g_2(\psi) + y^2)(\psi^2 g_0(0) + \frac{a^2}{y^2} g_2(0) + y^2)} . \quad (38)$$

In the ψ -integral the limit $a \rightarrow 0$ can be applied to the integrand, thereby eliminating g_2 and leading with (34) to

$$\int_{-\pi/4}^{\pi/4} d\psi \frac{2\psi^2 - 1 + \cos 2\psi}{(1 - \cos 2\psi + y^2)(2\psi^2 + y^2)} . \quad (39)$$

For $y = 0$ this integral is equal to $(\frac{4}{\pi} - 1)$. Using this in (38) we get

$$I_2 = \left(1 - \frac{4}{\pi}\right) \log a + \mathcal{O}(a^0) . \quad (40)$$

Now we proceed with I_1 . After performing the ψ -integration we get with (34),(35) and using the shorthand

$$k_{12} = |\vec{k}_1 - \vec{k}_2| , \quad (41)$$

as well as the substitution $r = \sqrt{\frac{a}{k_{12}}} \frac{2}{x}$ and the abbreviation

$$b = \frac{\sqrt{2ak_{12}}}{\pi} \quad (42)$$

$$I_1 = \frac{4}{\pi b} \int_{\frac{\sqrt{2\pi b}}{lk_{12}}}^{\infty} \arctan\left(\frac{x}{b\sqrt{1+x^4}}\right) \frac{dx}{\sqrt{1+x^4}} . \quad (43)$$

Obviously the leading divergent term for $b \rightarrow 0$ is given by

$$I_1^{\text{leading}} = \frac{4}{\pi b} \frac{\pi}{2} \int_0^{\infty} \frac{dx}{\sqrt{1+x^4}} . \quad (44)$$

To catch also the next-leading divergent term, we have to be more careful. With

$$I_1 = \frac{4}{\pi b} \hat{I}_1(b) \quad (45)$$

we find from (43)

$$\frac{d\hat{I}_1(b)}{db} = -\frac{\sqrt{2}\pi}{lk_{12}} \arctan\left(\frac{\sqrt{2}\pi}{lk_{12}}\right) (1 + \mathcal{O}(b^4)) - \int_{\frac{\sqrt{2\pi b}}{lk_{12}}}^{\infty} \frac{xdx}{x^2 + b^2(1+x^4)} . \quad (46)$$

The integral in the second term can be done explicitly, and we find altogether

$$\frac{d\hat{I}_1(b)}{db} = 2 \log b + \mathcal{O}(b^0) , \quad (47)$$

and after integration

$$\hat{I}_1(b) = \hat{I}_1(0) + 2b \log b + \mathcal{O}(b) . \quad (48)$$

Using this in (45) we get with (42) after evaluation of the integral in (44)

$$I_1 = \frac{\sqrt{\pi} (\Gamma(1/4))^2}{2 \sqrt{2ak_{12}}} + \frac{4}{\pi} \log a + \mathcal{O}(a^0) . \quad (49)$$

Combining this with (36), (40) the final result is

$$I(a, l, \vec{k}_1, \vec{k}_2) = \frac{\sqrt{\pi} (\Gamma(1/4))^2}{2 \sqrt{2a |\vec{k}_1 - \vec{k}_2|}} + \log a + \mathcal{O}(a^0) . \quad (50)$$

Appendix B

In the holographic calculation we have to handle (24), which after performing the r -integration becomes

$$A_\epsilon^\pm = -\frac{\tau_\epsilon^\pm}{r_0} \frac{(2\pi)^{3/2}}{(\Gamma(\frac{1}{4}))^2} + \int_{-\tau_\epsilon^\pm}^{\tau_\epsilon^\pm} d\tau \frac{F(-\frac{1}{4}, \frac{1}{2}, \frac{3}{4}, (\frac{r_\epsilon^\pm(\tau)}{r_0})^4)}{r_\epsilon^\pm(\tau)}. \quad (51)$$

In this formula, for each τ , $r_\epsilon^\pm(\tau)$ is a solution of

$$\epsilon \tau^2 = r_\epsilon^\pm(\tau) - \epsilon \left((M \pm \sigma(r_\epsilon^\pm(\tau)))^2 + (r_\epsilon^\pm(\tau))^2 \right). \quad (52)$$

The function $\sigma(r)$ is given by

$$\sigma(r) = r_0 \int_{r/r_0}^1 \frac{y^2 dy}{\sqrt{1-y^4}}, \quad (53)$$

and the boundaries of the τ -integration are fixed by that values of τ , which for given ϵ and $0 \leq r \leq r_0$ maximise the r.h.s. of (52). For the plus variant this happens at $r = r_0$ and for the minus variant at a value in the $\mathcal{O}(\epsilon)$ vicinity of r_0 .

$$\begin{aligned} \tau_\epsilon^+ &= \sqrt{\frac{r_0}{\epsilon} - (M^2 + r_0^2)}, \\ \tau_\epsilon^- &= \sqrt{\frac{r_0}{\epsilon} - (M^2 + r_0^2)} + \mathcal{O}(\epsilon). \end{aligned} \quad (54)$$

The integral in (51) becomes divergent since $r_\epsilon^\pm(\tau)$ goes to zero for $\epsilon \rightarrow 0$. The hypergeometric function in the nominator behaves as $1 + \mathcal{O}((r_\epsilon^\pm)^4)$. Therefore, using further (52), and putting $\tau = \alpha \tau_\epsilon^\pm$ we get

$$A_\epsilon^\pm = -\frac{\tau_\epsilon^\pm}{r_0} \frac{(2\pi)^{3/2}}{(\Gamma(\frac{1}{4}))^2} + \frac{1}{\epsilon \tau_\epsilon^\pm} \int_{-1}^1 \frac{d\alpha}{\alpha^2 + \frac{1}{(\tau_\epsilon^\pm)^2} ((M \pm \sigma(r_\epsilon^\pm(\tau)))^2 + (r_\epsilon^\pm(\tau))^2)} + \mathcal{O}(\epsilon^0). \quad (55)$$

The remaining integral is of the type $\int (\alpha^2 + \epsilon f(\alpha, \epsilon))^{-1} d\alpha$, its asymptotic estimate for $\epsilon \rightarrow 0$ is given by

$$\int_{-1}^1 \frac{d\alpha}{\alpha^2 + \epsilon f(\alpha, \epsilon)} = \frac{\pi}{\sqrt{\epsilon f(0, 0)}} - 2 + \mathcal{O}(\epsilon^{1/2}). \quad (56)$$

Using (54), we have in our case $f(0, 0) = \frac{(M \pm L/2)^2}{r_0}$. Then from (55) and the $r_0 \leftrightarrow L$ relation (16) we get finally

$$A_\epsilon^\pm = \frac{\pi}{\epsilon(M \pm L/2)} - \frac{2(2\pi)^{3/4}}{\Gamma(\frac{1}{4})} \left(1 + \frac{\pi\sqrt{2\pi}}{(\Gamma(\frac{1}{4}))^2} \right) \frac{1}{\sqrt{\epsilon L}} + \mathcal{O}(\epsilon^0). \quad (57)$$

Appendix C

The Wilson loop contour in section 3 is of self-touching type, the tips of two spikes coincide. To compare it with the result for an isolated spike in section 2 requires some comments.

As for self-crossing contours one has to expect mixing under renormalisation. In our case it would be mixing between W and \tilde{W} , where \tilde{W} is the correlator of the Wilson loops for the two single circles. The contour near our double spike with the arrows pointing in the direction of the colour flux and increasing contour parameter is shown in figure 4.



Figure 4: *Contour from section 3. To draw the flow of colour and contour parameter in an eye-catching manner, the common tip of the spikes has been splitted.*

The four legs are numerated as in the figure, and below the double index indicates between which legs the propagators run. As argued in section 2, cases where the propagator has both ends on the same leg have to be included only for those legs on which the arrow points away from the spiky point. Then we get

$$\log W = \frac{g^2 C_F}{4\pi^2} \left(\sum_{i,j} (I_{sc}^{ij} - I_{gl}^{ij}) + \dots \right) + \mathcal{O}(g^4) , \quad (58)$$

with

$$\begin{aligned} I_{sc}^{12} &= I_{sc}^{34} = \frac{B}{\sqrt{2ak_{12}}} + \log a , \\ I_{sc}^{22} &= I_{sc}^{44} = \log a , \\ I_{sc}^{13} &= I_{sc}^{14} = I_{sc}^{23} = I_{sc}^{24} = -\log a , \end{aligned} \quad (59)$$

and

$$\begin{aligned} I_{gl}^{12} &= I_{gl}^{34} = -\frac{B}{\sqrt{2ak_{12}}} - \log a , \\ I_{gl}^{22} &= I_{gl}^{44} = I_{gl}^{13} = I_{gl}^{24} = \log a , \\ I_{gl}^{14} &= I_{gl}^{23} = -\log a . \end{aligned} \quad (60)$$

Remarkably now, in contrast to the single spike case, the $\log a$ terms cancel both for the gluonic as well as the scalar terms. Then we get *both* for QCD and SYM a pure $1/\sqrt{a}$ divergence to be attributed to the touching spikes.

References

- [1] A. M. Polyakov, Nucl. Phys. B **164** (1980) 171.
- [2] V. S. Dotsenko and S. N. Vergeles, Nucl. Phys. B **169** (1980) 527.
- [3] S. J. Rey and J. T. Yee, Eur. Phys. J. C **22** (2001) 379 [hep-th/9803001].
- [4] J. M. Maldacena, Phys. Rev. Lett. **80** (1998) 4859 [hep-th/9803002].
- [5] N. Drukker, D. J. Gross and H. Ooguri, Phys. Rev. D **60** (1999) 125006 [hep-th/9904191].
- [6] R. A. Brandt, F. Neri and M. A. Sato, Phys. Rev. D **24** (1981) 879.
- [7] D. Knauss and K. Scharnhorst, Annalen Phys. **41** (1984) 331.
- [8] G. P. Korchemsky and A. V. Radyushkin, Nucl. Phys. B **283** (1987) 342.
- [9] D. Correa, J. Henn, J. Maldacena and A. Sever, JHEP **1205** (2012) 098 [arXiv:1203.1019 [hep-th]].
- [10] A. Grozin, J. M. Henn, G. P. Korchemsky and P. Marquard, Phys. Rev. Lett. **114** (2015) no.6, 062006 [arXiv:1409.0023 [hep-ph]].
- [11] V. Forini, A. A. Tseytlin and E. Vescovi, JHEP **1703** (2017) 003 [arXiv:1702.02164 [hep-th]].
- [12] B. Eden and M. Staudacher, J. Stat. Mech. **0611** (2006) P11014 [hep-th/0603157].
- [13] N. Beisert, B. Eden and M. Staudacher, J. Stat. Mech. **0701** (2007) P01021 [hep-th/0610251].
- [14] S. Ryu and T. Takayanagi, Phys. Rev. Lett. **96** (2006) 181602 [hep-th/0603001].
- [15] S. Ryu and T. Takayanagi, JHEP **0608** (2006) 045 [hep-th/0605073].
- [16] D. Correa, J. Henn, J. Maldacena and A. Sever, JHEP **1206** (2012) 048 [arXiv:1202.4455 [hep-th]].
- [17] N. Drukker and V. Forini, JHEP **1106** (2011) 131 [arXiv:1105.5144 [hep-th]].
- [18] H. Dorn, Fortsch. Phys. **34** (1986) 11.
- [19] A. M. Polyakov, Nucl. Phys. Proc. Suppl. **68** (1998) 1 [hep-th/9711002].
- [20] G. Pastras, arXiv:1710.01948 [hep-th].
- [21] H. Dorn, J. Phys. A **49** (2016) no.14, 145402 [arXiv:1509.00222 [hep-th]].
- [22] J. L. Gervais and A. Neveu, Nucl. Phys. B **163** (1980) 189.

- [23] I. Y. Arefeva, Phys. Lett. **93B** (1980) 347.
- [24] N. S. Craigie and H. Dorn, Nucl. Phys. B **185** (1981) 204.
- [25] S. Aoyama, Nucl. Phys. B **194** (1982) 513.
- [26] A. Dekel, JHEP **1701** (2017) 085 [arXiv:1610.07179 [hep-th]].
- [27] S. N. Solodukhin, Phys. Lett. B **665** (2008) 305 [arXiv:0802.3117 [hep-th]].
- [28] H. Dorn, Phys. Lett. B **763** (2016) 134 [arXiv:1608.04900 [hep-th]].
- [29] R. C. Myers and A. Singh, JHEP **1209** (2012) 013 [arXiv:1206.5225 [hep-th]].
- [30] I. R. Klebanov, T. Nishioka, S. S. Pufu and B. R. Safdi, JHEP **1207** (2012) 001 [arXiv:1204.4160 [hep-th]].